Available online at http://scik.org

Commun. Math. Biol. Neurosci. 2022, 2022:126

https://doi.org/10.28919/cmbn/7776

ISSN: 2052-2541

DETECTION OF PULMONARY TUBERCULOSIS FROM CHEST X-RAY IMAGES USING MULTIMODAL ENSEMBLE METHOD

JIMMY[1,*], TJENG WAWAN CENGGORO[2,3], BENS PARDAMEAN[1,3], JULIANA GOZALI[4], DENNY TANUMIHARDJA[4]

[1]Computer Science Department, BINUS Graduate Program-Master of Computer Science Program, Bina Nusantara University, Jakarta 11480, Indonesia

[2]Computer Science Department, School of Computer Science, Bina Nusantara University, Jakarta 11480, Indonesia

[3]Bioinformatics and Data Science Research Center, Bina Nusantara University, Jakarta 11480, Indonesia

[4]Radiology Department, Murni Teguh Memorial Hospital, Medan 20231, Indonesia

Abstract: Tuberculosis (TB) is one of the deadliest diseases nowadays, and it is caused by the mycobacterium tuberculosis bacterium that generally attacks the lungs. Following artificial intelligence implementation in the field of computer vision, especially deep learning, many computer-based diagnostic systems have been proposed to help detect TB from chest X-Ray images. It can produce better and faster accuracy and consistency of the diagnosis results. However, many radiology applications based on the deep learning method consider only images as input sources. In modern medical practice, non-imaging data from patient medical record history or patient demographics may influence disease detection and provide more data for radiologists to obtain additional insights in a clinical context. This study proposed a multimodal model that uses images and patient demographics to answer the need. The evaluation results show that our approach leads to high accuracy and can improve the area under curve (AUC) value by 0.0213 compared to the unimodal model. Additionally, this model successfully outperformed the previous state-of-the-art multimodal model by a 0.0075 (0.0213 vs. 0.0138, respectively) increase in AUC.

*Corresponding author

E-mail address: jimmy012@binus.ac.id

Received October 10, 2022

Keywords: tuberculosis; deep learning; computer vision; multimodal; ensemble.

2010 AMS Subject Classification: 93A30, 65D18.

1. INTRODUCTION

Tuberculosis (TB) is a global health problem, and Indonesia is among the top 3 countries with the most TB sufferers, after India and China [1]. According to the Indonesia Healthcare insurances report 2018, TB is in the top 5 diseases besides hypertension, stroke, heart failure, and diabetes. It is a disease that has long attacked humans and is still a high cause of death worldwide. Although TB is a curable disease, the key to a patient's recovery is timely diagnosis and treatment. Consequently, a delay in diagnosis can reduce the patient's chances of recovery [2]. With many TB patients requiring rapid treatment, early screening is vital in adequately managing patients. One of the initial screening techniques to identify TB is through X-Ray thorax images. From these X-Ray images, radiologists can locate the type of infection that occurs in the patient. However, new problems have emerged from this approach, as radiologists may experience fatigue, burn-out, and an increase in error rate due to the large number of images that need to be examined [3]. Therefore, a computer-based diagnostic system is highly recommended to ease radiologists' workload. This system can produce outstanding accuracy and consistency in diagnosis [4]. Previous studies have developed various diagnostic systems to predict TB based on conventional machine learning or deep learning [5]–[8].

Several previous studies have proven the deep learning method effective in TB classification tasks. Nevertheless, the models used in these studies only took images as input without leveraging other clinical data such as patient demographics, chest abnormalities, laboratory test results, or patient assessments as done in real-world clinical practices. A past survey found that radiologists require clinical information when interpreting images, which would impact their reports and patient clinical outcomes [9]. Thus, to answer the problems mentioned earlier, we proposed a

technique in which images and patient demographic data are leveraged in a multimodal ensemble model to solve complex TB classification tasks. This model adopts EfficientNet [10] and XGBoost [11] as the base model and is followed by a weighted ensemble to generate final predictions. Experiments were carried out on a dataset taken from Murni Teguh Memorial Hospital, Medan, Indonesia.

2. RELATED WORKS

Historically, computer-based systems for TB diagnosis relied heavily on feature extraction and pattern recognition techniques. With its emergence and rising popularity, CNNs have been applied in many pulmonary TB classification studies [7], [8], [12]. CNN is a data-hungry network. Unfortunately, most medical imaging datasets are often tiny and may not provide enough data to train this network from scratch. In medical image research, transfer learning is currently the most popular approach in attempting to improve the deep learning model. It enables the CNN model to learn effectively from small datasets and enhance accuracy and time consumption[13]–[21]. Muljo, Pardamean, Purwandari, and Cenggoro suggested a transfer learning technique that used pre-trained DenseNet121 in their lung disease classification study, which achieved a decent AUC of 99.99% [22]. Besides transfer learning, image segmentation is another technique to improve the TB detection model. This technique was used to extract lung regions from chest X-Ray images [23], [24]. Not only medical images, but image segmentation can also work well on other computer vision tasks not involving medical, as demonstrated by Muchtar, Rahman, Cenggoro, Budiarto, and Pardamean, which proposed a texture-based foreground segmentation using a block-based adaptive segmenter method [25]. Furthermore, this concept was also used to develop an intelligent human counting system for smart building management [26].

2.1 TB detection using Ensemble of CNN

Only one model is applied in most CNN applications, especially in a classification task. However, there is an approach to using multiple CNN models to solve the same problem called an

ensemble, which is the technique that uses various CNN algorithms to get a better predictive result [27], [28]. As a result, ensemble techniques have attracted machine learning researcher's attention. Guo, Passi, and Jain introduced an ensemble method that combines multiple CNN models, which included VGG16 [29], VGG19 [29], InceptionV3 [30], ResNet34, ResNet50, and ResNet101 to produce 0.99 of AUC in their research for chest abnormalities [31].

2.2 EfficientNet on classification tasks

EfficientNet was first introduced by Tan and Le [10]. This model approach applies compound scaling in all network dimensions, such as width, depth, and image resolution. The performance of EfficientNet had reached state-of-the-art on the Imagenet while being 8.4x smaller and 6.1x faster [10]. Due to excellent accuracy and time efficiency, Munadi, Muchtar, Maulina, and Pradhan used EfficientNet in their TB detection study [32]. More recently, Marques, Agarwal, and de la Torre Díez [33] suggest an automatic medical diagnosis of COVID-19 using EfficientNet [33]. Although mainly used for image classification tasks, EfficientNet had also obtained magnificent results in sounds classification tasks. Gunawan, Hidayat, Cenggoro, and Pardamean demonstrated EfficientNet model used two acoustic features to classify owl sound. As such, it can be said that its prowess in deep learning-related tasks has undoubtedly been astounding [34].

2.3 XGBoost for disease diagnosis

Unlike the previous CNN model based on deep learning, the XGBoost Algorithm is the advanced gradient boosting method based on a tree algorithm. One of this method's advantages is handling regularization and overfitting-underfitting issues. Budholiya, Shrivastava, and Sharma used this model in their heart disease prediction study [35]. On the other hand, Li, Fu, and Li used an XGBoost algorithm for diabetes prediction [36]. These studies showed that XGBoost worked very well when used to train tabular medical data. Another technique to leverage XGBoost for TB detection was introduced by Rahman, Cao, Sun, Li, and Hao [37]. The technique used in their study is to replace the fully connected layer on CNN with XGBoost for classification tasks.

2.4 Multimodal model for TB detection

As mentioned earlier in section 1, modern medical practice relies heavily on multiple data sources, where substantial clinical context is often essential for making diagnostic decisions. Therefore, Heo et al. [40] presented a multimodal technique that leveraged image data and demographics variables, including age, gender, height, and weight, for their TB classification model. Before training, image segmentation was applied in the preprocessing step using the U-Net [38] algorithm. This multimodal model has successfully increased an AUC score by 0.0138 compared to the non-demographic variables model.

3. METHODS AND MATERIALS

3.1 Ethics Statement

Private medical records for all patients were anonymized before analysis. Murni Teguh Memorial Hospital Medan, Indonesia, and the Health Research Ethical Committee of Medical Faculty Nommensen HKBP University Medan, Indonesia, has approved this study (IRB: 256/KEPK/FK/VII/2021).

3.2 Dataset

The training dataset used in this study is a collection of images and demographic variables from 2014 to 2021 as part of Murni Teguh Memorial Hospital's daily radiology examination routines. A total of 754 images, which consists of 552 normal X-Ray images and 202 images of TB used in this study. This study used demographic variables included age, sex, and body mass index (BMI). Past studies have shown that underweight patient have a higher infection rate compared to a patient with an average weight (1.80 vs. 0.92 per 1000 patients) [39]. We allocated 20% of training data for validation purposes. In addition, a separate dataset was distributed for testing purposes, consisting of 47 normal images and 47 pulmonary TB images. It is worth mentioning that testing datasets were not used in the training phase of the model and all training and testing datasets have the corresponding radiologist examination report, which is then considered ground truth.

3.3 Method

The proposed method is shown in Figure 1. EfficientNet was used for image classification, while XGBoost [11] was used for demographic variables classification.

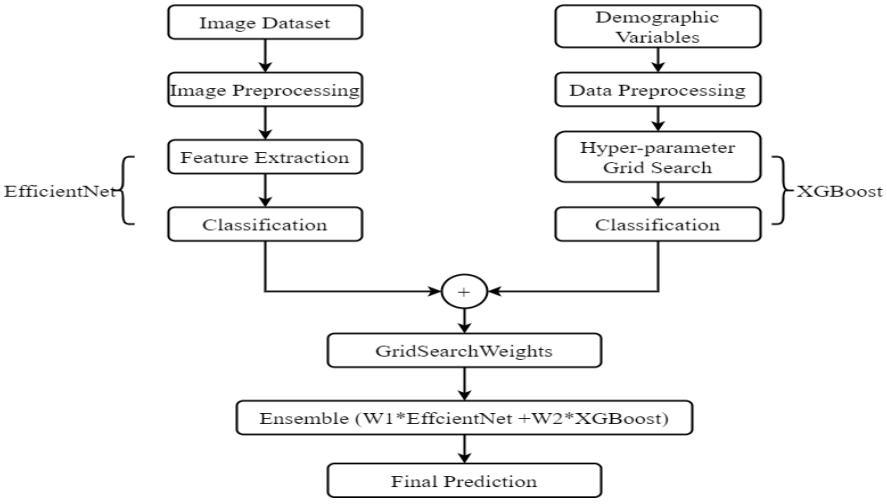

Figure 1. Multimodal ensemble method for TB detection

The image dataset contains two types of images: non-segmented and segmented images. We used the U-Net model to generate the image masks. This model was previously trained using two public datasets, namely Shenzhen and Montgomery, which achieved a dice coefficient of 0.9633 for 138 test sets. Following this, we applied the bitwise operation to crop only part of the lung corresponding to the mask after they were generated, as shown in Figure 2.

Figure 2. Lung Segmentation Using U-Net and OpenCV Bitwise Operation.

All input images were resized to 260 x 260 pixels prior to training. As mentioned earlier in section 2, one advantage of transfer learning is its capability to be used for small datasets. Realizing that our dataset is small, we used pre-trained ImageNet weights for EfficientNet in this study. During the evaluation, the EfficientNet models used are EfficientNetB1-B5. Lastly, we add the following custom top layers: Global Average Pooling layer, Fully Connected layer, Batch

Normalization layer, Dropout layer, and Sigmoid Classification layer. The details of each layer can be seen in Table 1.

Demographic variables consisting of age, gender, and BMI used in this study were raw data. To handle this, we used data preprocessing methods such as null value filling, one-hot (OH) encoding, and row-grouping. Our strategy applied one-hot encoding to age, gender, and BMI, then trained these variables using the XGBoost model.

As mentioned earlier in Figure 1, this study proposed a multimodal ensemble architecture of deep learning and machine learning algorithms to detect TB from CXR images. Therefore the final step in this method is to use each individually predicted result as input for the weighted ensemble model, as shown in (1):

$$Pred = w_1 \times \hat{y}_1 + w_2 \times \hat{y}_2 \qquad (1)$$

Equation (1) contains variables $\hat{y}_1$ and $\hat{y}_2$, which are predictions of EffcientNet and the XGBoost model. Additionally, both w_1 and w_2 are weight parameters for those models.

Table 1. EfficientNet Layer Types and Parameters Used in Proposed Method.

Layer (Type)	Input_shape	Output_shape
Image_input	260x260x3	260x260x3
top_conv	9x9x352	9x9x1408
top_bn	9x9x1408	9x9x1408
top_activation	9x9x1408	9x9x1408
dropout	9x9x1408	9x9x1408
global_avg_pool	9x9x1408	1408
pred (dense)	1408	1

The contribution made by this study was introducing an ensemble model that can use multiple sources of input to solve TB classification tasks. We also compared the final proposed method with the previous state-of-the-art multimodal model by Heo et al. The results demonstrated that this study method obtained a better performance.

4. RESULTS AND DISCUSSION

4.1 Demographic Variables with XGBoost

The first step in the method is to train the XGBoost model using demographic variables consisting of one categorical variable, gender, and two numeric variables: age and BMI. Before training, row grouping, and one-hot encoding were done for age, gender, and BMI. The detail of demographic variables categorization can be seen in Table 2 and Table 3.

Table 2. BMI Classifications.

Classification	BMI
Underweight	< 18.5
Normal	18.5-25.0
Overweight	25.1-27.0
Obese	> 27

Table 3. Age Grouping.

Group	Age	
	From	To
1	0	5
2	6	11
3	12	16
4	17	25
5	26	35
6	36	45
7	45	56
8	56	65
9	> 65	

Since XGBoost is a decision tree-based algorithm, multiple tree-related hyper-parameters, including n_estimator, max_depth, and learning_rate, were used to improve the model performance. These hyper-parameters and their description are shown in Table 4.

Table 4. XGBoost Classifier Parameters.

Parameters	Default value	Description
n_estimators	500	Number of trees to fit
max_depth	4	Maximum depth of the tree
learning_rate	0.05	Shrink the weight on each step

Two kinds of experiments were utilized on demographic variables. Firstly, the XGBoost classifier was used on gender and BMI, and then we applied it to age, gender, and BMI. Both were preprocessed using one-hot-encode, and the performance evaluation of XGBoost is shown in Table 5.

Table 5. Demographic Variables with XGBoost.

n_estimator	max_depth	LR	AUC	Specificity	Sensitivity
gender and BMI one-hot encoded					
500	4	0.05	0.8512	0.8723	0.5531
500	4	0.025	0.8723	0.8723	0.5106
500	4	0.0125	0.8843	0.8723	0.5957
500	4	0.00625	0.8940	0.8936	0.5744
500	8	0.05	0.8327	0.8510	0.6170
500	8	0.025	0.8435	0.8510	0.6170
500	8	0.0125	0.8626	0.8723	0.5957
500	8	0.00625	0.8707	0.8723	0.6808
age, gender, and BMI one-hot encoded					
500	4	0.05	0.8838	0.9361	0.6170
500	4	0.025	0.8807	0.8936	0.6170
500	4	0.0125	0.8684	0.9361	0.5531
500	4	0.00625	0.8644	0.9361	0.5531
500	8	0.05	0.8829	0.8931	0.6170
500	8	0.025	0.8811	0.8936	0.6170
500	8	0.0125	0.8798	0.8936	0.6170
500	8	0.00625	0.8798	0.8936	0.6170

4.2 Non Segmented Image + Demographics variable performance

Next is to train non-segmented images and ensemble them with demographic variables to get the final result. As mentioned earlier in section 3.1, the CNNs model used were five versions of EfficientNet from B1 to B5. In addition, according to the previous XGBoost result, there are two variations of the ensemble model. The first is the demographics variable with one-hot encoded on gender and BMI, and the second is demographics with one-hot encoded on age, gender, and BMI. Ensemble results of this model can be seen in Table 6. The best performance is marked with **bold** font.

Table 6. Non-segmented Image Model Performance with Gender and BMI One-hot Encoded.

Models	Image without Segmentation		
	Threshold (0.5)		
	CNN	CNN+DV[1]	AUC Difference
EfficientNet-B1	0.8829	0.8829	0.0000
EfficientNet-B2	0.9361	0.9468	**0.0107**
EfficientNet-B3	0.9148	0.9255	0.0107
EfficientNet-B4	0.8829	0.8829	0.0000
EfficientNet-B5	0.9148	0.9148	0.0000

[1]CNN with demographic variables

To determine the best multimodal model, we compare AUC values for the CNN model using only images and CNN with the XGBoost ensemble technique. AUC values for EfficientNetB1-B5 in the test set before ensemble were 0.8829, 0.9361, 0.9148, 0.8829, and 0.9148 respectively. Through an ensemble process, this model successfully increased the AUC value by 0.0107. Thus, we added preprocessed age variables to the model with the same training step as the previous model. These resulted in an increment of the AUC value by 0.0213, as shown in Table 7.

Table 7. Non-segmented Image Model Performance with Age, Gender, and BMI One-hot Encoded.

Models	Image without Segmentation		
	Threshold (0.5)		
	CNN	CNN+DV[1]	AUC Difference
EfficientNet-B1	0.8829	0.8829	0.0000
EfficientNet-B2	0.9361	**0.9574**	**0.0213**
EfficientNet-B3	0.9148	0.9255	0.0107
EfficientNet-B4	0.8829	0.9042	0.0213
EfficientNet-B5	0.9148	0.9148	0.0000

[1]CNN with demographics variable

4.3 Segmented Image + Demographics variable performance

This model aims to discover if a segmented image has better results than the non-segmented image model. Results by model leveraging segmented image combined with the demographics variable model can be seen in Table 8 and Table 9.

Table 8. Segmented Image Performance with Gender and BMI One-hot Encoded.

Models	Image with Segmentation		
	Threshold (0.5)		
	CNN	CNN+DV[1]	AUC Difference
EfficientNet-B1	0.8723	0.8723	0.0000
EfficientNet-B2	0.9042	0.9148	**0.0106**
EfficientNet-B3	0.9148	0.9148	0.0000
EfficientNet-B4	0.8936	0.9042	0.0106
EfficientNet-B5	0.9361	0.9361	0.0000

[1]CNN with demographic variables

Table 9. Segmented Image Performance with Age, Gender, and BMI One-hot Encoded.

Models	Image with Segmentation		
	Threshold (0.5)		
	CNN	CNN+DV[1]	AUC Difference
EfficientNet-B1	0.8723	0.8936	**0.0213**
EfficientNet-B2	0.9042	0.9148	0.0106
EfficientNet-B3	0.9148	0.9255	0,0107
EfficientNet-B4	0.8936	0.9042	0.0106
EfficientNet-B5	0.9361	0.9361	0.0000

[1]CNN with demographic variables

Considering the experimental results above, we have analyzed the causes of an increase in AUC by calculating the difference in specificity and sensitivity values. Figure 2 shows the confusion matrix for the EficientNet-B2 network without demographic variables, and Figure 3 shows the confusion matrix for the multimodal model with demographic variables. There is a change in the number of false positives and false negatives after applied demographic variables.

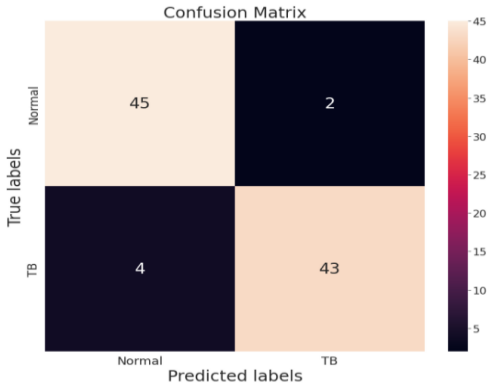

Figure 2. Confusion Matrix for Unimodal Model.

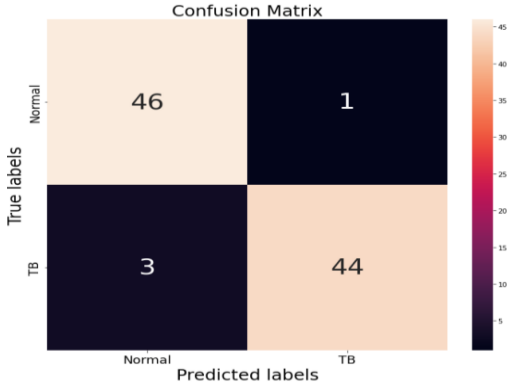

Figure 3. Confusion Matrix for Multimodal Model.

A further analysis was conducted to examine the difference in the sensitivity and specificity of unimodal and multimodal models. The multimodal model showed greater sensitivity and specificity reflected in 0.9361 and 0.9574, respectively. The ROC Curve of the multimodal ensemble can be seen in Figure 4.

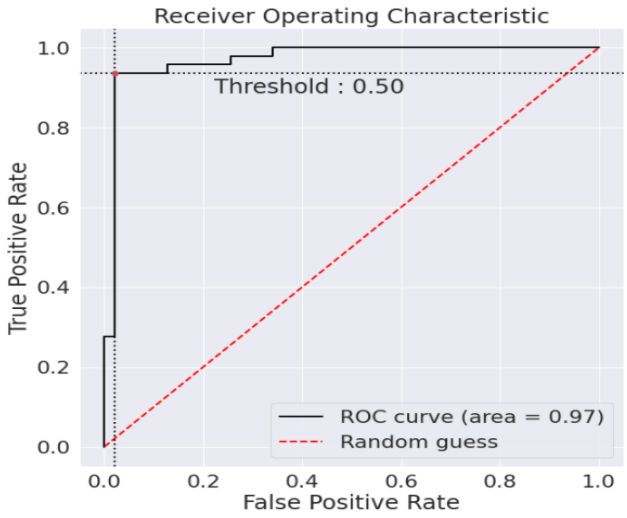

Figure 4. Receiver Operating Characteristic (ROC) Curve of Multimodal Ensemble.

4.4 Results using a previous multimodal method

Based on different datasets used on the previous multimodal model by Heo et al., we have replicated their model for evaluation on our datasets. A comparative analysis was done based on the AUC value in Table 10. The greater AUC was recorded in the image without segmentation. These outcomes align with the results of our methods that show higher AUC in non-segmented images as well. The performance shown in Table 10 indicates that the best AUC obtained by the previous model is 0.9255, compared to 0.9574 using our proposed model.

Table 10. Heo et al. (2019) Model Results on Study Dataset

Models	AUC		
	CNN	CNN+DV[1]	Difference
Heo et al. (2019) model without image segmentation	0.9148	0.9255	0.0107
Heo et al. (2019) model with image segmentation	0.9042	0.9148	0.0106

5. DISCUSSIONS

The experimental results illustrate that combining EfficientNet and XGBoost impacts the model performance. In Rahman, Cao, Sun, Li, and Hao's [37] study, they achieved a better AUC of 99.43 ± 0.39% using VGG19-XGBoost. On the other hand, our model outperforms the model proposed by Munadi, Muchtar, Maulina, and Pradhan [32] in AUC (0.9574 vs. 0.9480). However, their model is not a multimodal model like our proposed method, making it improper to perform a comparison, and that is not apple-to-apple.

According to the experimental results, EfficientNetB2-XGBoost has the best performance with 0.9574 AUC and 0.0213 points increment. Meanwhile, our final multimodal model outperforms the previous study regarding AUC and its increment when combined with demographic variables. Table 11 shows a comparison of AUC values to our proposed method, and the best performance is marked with **bold** font.

Table 11. Comparison between Proposed and Benchmark Models.

Models	CNN-AUC	CNN+DV[1]-AUC	Difference
Heo et al. (2019)	0.9075	0.9213	0.0138
Proposed Model	**0.9361**	**0.9574**	**0.0213**

[1]CNN with demographic variables

6. CONCLUSIONS

The primary goal of this study was to improve the TB detection model with additional demographic variables. The present study proved that this model could improve the AUC values by 0.0213 points, and this study method also proved that proper demographic variables preprocessing will enhance detection performance. As shown in Table 6 and Table 7, an AUC of 0.0106 points increases compared to the non-grouped age model. Our model works well with a modern medical method that heavily depends on numerous data sources to support decision-making. Based on the experimental results, we can conclude that the suggested approach can

improve the quality of TB diagnosis. This also opens the possibility for future works to develop a robust model with other medical data sources such as laboratory reports, patient assessment records, and radiology examination reports.

ACKNOWLEDGEMENTS

This work was supported by Murni Teguh Memorial Hospital, Medan, Indonesia, in association with Bioinformatics and Data Science Research Center, Bina Nusantara University, Jakarta, Indonesia.

We would like to thank Gregorius Natanael Elwirehardja and Digdo Sudigyo for their guidance in improving the manuscript writing. We also thank Bambang Eko Santoso for the helpful discussion during the development of the study.

CONFLICT OF INTERESTS

The author(s) declare that there is no conflict of interests.

REFERENCES

[1] J. Gozali, D. Tanumihardja, S. S. Widjaja, et al. Chest X-Ray findings in pulmonary tuberculosis with and without comorbid diseases, Eur. Congress Radiol. ECR 2019 (2019), C-2325. https://doi.org/10.26044/ECR2019/C-2325.

[2] A. Yahiaoui, O. Er, N. Yumusak, A new method of automatic recognition for tuberculosis disease diagnosis using support vector machines, Biomed. Res. 28 (2017), 4208–4212. https://hdl.handle.net/20.500.12619/2466.

[3] S.C. Huang, A. Pareek, S. Seyyedi, I. Banerjee, M.P. Lungren, Fusion of medical imaging and electronic health records using deep learning: a systematic review and implementation guidelines, Npj Digit. Med. 3 (2020), 136. https://doi.org/10.1038/s41746-020-00341-z.

[4] W.Y. Nyein Naing, Z. Z. Htike, Advances in automatic tuberculosis detection in chest X-Ray images, Signal Image Process. 5 (2014), 41–53. https://doi.org/10.5121/sipij.2014.5604.

[5] A. Chauhan, D. Chauhan, C. Rout, Role of gist and PHOG features in computer-aided diagnosis of tuberculosis without segmentation, PLoS ONE. 9 (2014), e112980. https://doi.org/10.1371/journal.pone.0112980.

[6] S. Vajda, A. Karargyris, S. Jaeger, et al. Feature selection for automatic tuberculosis screening in frontal chest

radiographs, J. Med. Syst. 42 (2018), 146. https://doi.org/10.1007/s10916-018-0991-9.

[7] S. Sathitratanacheewin, P. Sunanta, K. Pongpirul, Deep learning for automated classification of tuberculosis-related chest X-Ray: dataset distribution shift limits diagnostic performance generalizability, Heliyon. 6 (2020), e04614. https://doi.org/10.1016/j.heliyon.2020.e04614.

[8] M. Oloko-Oba, S. Viriri, Diagnosing tuberculosis using deep convolutional neural network, in: A. El Moataz, D. Mammass, A. Mansouri, F. Nouboud (Eds.), Image and Signal Processing, Springer International Publishing, Cham, 2020: pp. 151–161. https://doi.org/10.1007/978-3-030-51935-3_16.

[9] W.W. Boonn, C.P. Langlotz, Radiologist use of and perceived need for patient data access, J. Digit. Imaging. 22 (2008), 357–362. https://doi.org/10.1007/s10278-008-9115-2.

[10] M. Tan, Q.V. Le, EfficientNet: Rethinking model scaling for convolutional neural networks, in: 36th Int. Conf. Mach. Learn. (ICML 2019), vol. 2019-June, pp. 10691–10700, 2019. https://doi.org/10.48550/arXiv.1905.11946.

[11] T. Chen, C. Guestrin, XGBoost: A scalable tree boosting system, in: Proceedings of the 22nd ACM SIGKDD International Conference on Knowledge Discovery and Data Mining, ACM, San Francisco California USA, 2016: pp. 785–794. https://doi.org/10.1145/2939672.2939785.

[12] M.E. Colombo Filho, R. Mello Galliez, F. Andrade Bernardi, et al. Preliminary results on pulmonary tuberculosis detection in chest X-Ray using convolutional neural networks, in: V.V. Krzhizhanovskaya, G. Závodszky, M.H. Lees, J.J. Dongarra, P.M.A. Sloot, S. Brissos, J. Teixeira (Eds.), Computational Science – ICCS 2020, Springer, Cham, 2020: pp. 563–576. https://doi.org/10.1007/978-3-030-50423-6_42.

[13] F.R. Lumbanraja, B. Mahesworo, T.W. Cenggoro, et al. An evaluation of deep neural network performance on limited protein phosphorylation site prediction data, Procedia Computer Sci. 157 (2019), 25–30. https://doi.org/10.1016/j.procs.2019.08.137.

[14] F.R. Lumbanraja, B. Mahesworo, T.W. Cenggoro, et al. SSMFN: a fused spatial and sequential deep learning model for methylation site prediction, PeerJ Computer Sci. 7 (2021), e683. https://doi.org/10.7717/peerj-cs.683.

[15] S.S. Meraj, R. Yaakob, A. Azman, et al. Detection of pulmonary tuberculosis manifestation in chest X-Rays using different convolutional neural network (CNN) models, Int. J. Eng. Adv. Technol. 9 (2019), 2270–2275. https://doi.org/10.35940/ijeat.a2632.109119.

[16] B. Pardamean, T.W. Cenggoro, R. Rahutomo, et al. Transfer learning from chest X-Ray pre-trained convolutional neural network for learning mammogram data, Procedia Computer Sci. 135 (2018) 400–407. https://doi.org/10.1016/j.procs.2018.08.190.

[17] N. Dominic, Daniel, T.W. Cenggoro, et al. Transfer learning using inception-ResNet-v2 model to the augmented neuroimages data for autism spectrum disorder classification, Commun. Math. Biol. Neurosci., 2021 (2021), 39.

https://doi.org/10.28919/cmbn/5565.

[18] T.W. Cenggoro, F. Tanzil, A.H. Aslamiah, et al. Crowdsourcing annotation system of object counting dataset for deep learning algorithm, IOP Conf. Ser.: Earth Environ. Sci. 195 (2018), 012063. https://doi.org/10.1088/1755-1315/195/1/012063.

[19] R. Rahutomo, A.S. Perbangsa, Y. Lie, et al. Artificial intelligence model implementation in web-based application for pineapple object counting, in: 2019 International Conference on Information Management and Technology (ICIMTech), IEEE, Jakarta/Bali, Indonesia, 2019: pp. 525–530. https://doi.org/10.1109/ICIMTech.2019.8843741.

[20] M. Norval, Z. Wang, Y. Sun, Pulmonary tuberculosis detection using deep learning convolutional neural networks, in: Proceedings of the 3rd International Conference on Video and Image Processing, ACM, Shanghai China, 2019: pp. 47–51. https://doi.org/10.1145/3376067.3376068.

[21] A.T. Sahlol, M. Abd Elaziz, A. Tariq Jamal, et al. A novel method for detection of tuberculosis in chest radiographs using artificial ecosystem-based optimisation of deep neural network features, Symmetry. 12 (2020), 1146. https://doi.org/10.3390/sym12071146.

[22] H.H. Muljo, B. Pardamean, K. Purwandari, et al. Improving lung disease detection by joint learning with COVID-19 radiography database, Commun. Math. Biol. Neurosci. 2022 (2022), 1. https://doi.org/10.28919/cmbn/6838.

[23] S. Gite, A. Mishra, K. Kotecha, Enhanced lung image segmentation using deep learning, Neural Comput Appl. (2022). https://doi.org/10.1007/s00521-021-06719-8.

[24] S. Rajaraman, L.R. Folio, J. Dimperio, et al. Improved semantic segmentation of tuberculosis—consistent findings in chest X-Rays using augmented training of modality-specific U-net models with weak localizations, Diagnostics. 11 (2021), 616. https://doi.org/10.3390/diagnostics11040616.

[25] K. Muchtar, F. Rahman, T.W. Cenggoro, et al. An improved version of texture-based foreground segmentation: Block-based adaptive segmenter, Procedia Computer Sci. 135 (2018), 579–586. https://doi.org/10.1016/j.procs.2018.08.228.

[26] B. Pardamean, H.H. Muljo, T.W. Cenggoro, B.J. Chandra, R. Rahutomo, Using transfer learning for smart building management system, J. Big Data. 6 (2019), 110. https://doi.org/10.1186/s40537-019-0272-6.

[27] P. Lakhani, B. Sundaram, Deep learning at chest radiography: Automated classification of pulmonary tuberculosis by using convolutional neural networks, Radiology. 284 (2017), 574–582. https://doi.org/10.1148/radiol.2017162326.

[28] S.K.T. Hwa, M.H.A. Hijazi, A. Bade, et al. Ensemble deep learning for tuberculosis detection using chest X-Ray

and canny edge detected images, IAES Int. J. Artif. Intell. 8 (2019), 429–435. https://doi.org/10.11591/ijai.v8.i4.pp429-435

[29] K. Simonyan, A. Zisserman, Very deep convolutional networks for large-scale image recognition, in: 3rd Int. Conf. Learn. Represent. ICLR 2015 - Conf. Track Proc., pp. 1–14, 2015.

[30] C. Szegedy, S. Ioffe, V. Vanhoucke, et al. Inception-v4, inception-ResNet and the impact of residual connections on learning, in: 31st AAAI Conf. Artif. Intell. AAAI 2017, pp. 4278–4284, 2017.

[31] R. Guo, K. Passi, C.K. Jain, Tuberculosis Diagnostics and Localization in Chest X-Rays via Deep Learning Models, Front. Artif. Intell. 3 (2020), 583427. https://doi.org/10.3389/frai.2020.583427.

[32] K. Munadi, K. Muchtar, N. Maulina, et al. Image Enhancement for tuberculosis detection using deep learning, IEEE Access. 8 (2020), 217897–217907. https://doi.org/10.1109/access.2020.3041867.

[33] G. Marques, D. Agarwal, I. de la Torre Díez, Automated medical diagnosis of COVID-19 through EfficientNet convolutional neural network, Appl. Soft Comput. 96 (2020), 106691. https://doi.org/10.1016/j.asoc.2020.106691.

[34] K.W. Gunawan, A.A. Hidayat, T.W. Cenggoro, et al. A Transfer Learning Strategy for Owl Sound Classification by Using Image Classification Model with Audio Spectrogram, Int. J. Electric. Eng. Inform. 13 (2021), 546–553. https://doi.org/10.15676/ijeei.2021.13.3.3.

[35] K. Budholiya, S.K. Shrivastava, V. Sharma, An optimized XGBoost based diagnostic system for effective prediction of heart disease, J. King Saud Univ. - Computer Inform. Sci. 34 (2022), 4514–4523. https://doi.org/10.1016/j.jksuci.2020.10.013.

[36] M. Li, X. Fu, D. Li, Diabetes prediction based on XGBoost algorithm, IOP Conf. Ser.: Mater. Sci. Eng. 768 (2020), 072093. https://doi.org/10.1088/1757-899x/768/7/072093.

[37] M. Rahman, Y. Cao, X. Sun, et al. Deep pre-trained networks as a feature extractor with XGBoost to detect tuberculosis from chest X-ray, Computers Electric. Eng. 93 (2021), 107252. https://doi.org/10.1016/j.compeleceng.2021.107252.

[38] O. Ronneberger, P. Fischer, T. Brox, U-Net: Convolutional networks for biomedical image segmentation, in: N. Navab, J. Hornegger, W.M. Wells, A.F. Frangi (Eds.), Medical Image Computing and Computer-Assisted Intervention-MICCAI 2015, Springer International Publishing, Cham, 2015: pp. 234–241. https://doi.org/10.1007/978-3-319-24574-4_28.

[39] H. Choi, J.E. Yoo, K. Han, et al. Body mass index, diabetes, and risk of tuberculosis: A retrospective cohort study, Front. Nutr. 8 (2021), 739766. https://doi.org/10.3389/fnut.2021.739766.

[40] S.J. Heo, Y. Kim, S. Yun, et al. Deep learning algorithms with demographic information help to detect

tuberculosis in chest radiographs in annual workers' health examination data, Int. J. Environ. Res. Public Health. 16 (2019), 250. https://doi.org/10.3390/ijerph16020250.